*Neuroimage*. Author manuscript; available in PMC 2016 December 19.

Published in final edited form as:

*Neuroimage*. 2015 April 15; 110: 110–123. doi:10.1016/j.neuroimage.2015.01.050.

# Comparing cerebrovascular reactivity measured using BOLD and cerebral blood flow MRI: The effect of basal vascular tension on vasodilatory and vasoconstrictive reactivity

**Sheliza Halani**[a], **Jonathan B. Kwinta**[a,b], **Ali M. Golestani**[a], **Yasha B. Khatamian**[a], and **J. Jean Chen**[a,b,*]

[a]Rotman Research Institute, Baycrest Centre, Canada

[b]Department of Medical Biophysics, University of Toronto, Canada

## Abstract

Cerebrovascular reactivity (CVR) is an important metric of cerebrovascular health. While the BOLD fMRI method in conjunction with carbon-dioxide ($CO_2$) based vascular manipulation has been the most commonly used, the BOLD signal is not a direct measure of vascular changes, and the use of arterial-spin labeling (ASL) cerebral blood flow (CBF) imaging is increasingly advocated. Nonetheless, given the differing dependencies of BOLD and CBF on vascular baseline conditions and the diverse $CO_2$ manipulation types currently used in the literature, knowledge of potential biases introduced by each technique is critical for the interpretation of CVR measurements. In this work, we use simultaneous BOLD-CBF acquisitions during both vasodilatory (hypercapnic) and vasoconstrictive (hypocapnic) stimuli to measure CVR. We further imposed different levels of baseline vascular tension by inducing hypercapnic and hypocapnic baselines, separately from normocapnia by 4 mm Hg. We saw significant and diverse dependencies on vascular stimulus and baseline condition in both BOLD and CBF CVR measurements: (i) BOLD-based CVR is more sensitive to basal vascular tension than CBF-based CVR; (ii) the use of a combination of vasodilatory and vasoconstrictive stimuli maximizes the sensitivity of CBF-based CVR to vascular tension changes; (iii) the BOLD and CBF vascular response delays are both significantly lengthened at predilated baseline. As vascular tension can often be altered by potential pathology, our findings are important considerations when interpreting CVR measurements in health and disease.

### Keywords

Cerebrovascular reactivity (CVR); Blood-oxygenation level-dependent signal (BOLD); Cerebral blood flow (CBF); Arterial-spin labeling (ASL); Hypercapnia; Hypocapnia; Vasodilation; Vasoconstriction; Prospective targeting

*Corresponding author at: Rotman Research Institute, Baycrest, 3560 Bathurst Street, Toronto, Ontario M6A 2E1, Canada. jchen@research.baycrest.org (J.J. Chen).

**Conflict of interest**

The authors declare no conflict of interest.

## Introduction

Cerebrovascular reactivity (CVR) is an important metric of cerebrovascular health. Experimentally, CVR is defined as the degree of vasodilatation or constriction in response to a vasoactive agent or task. CVR is an indication of vascular reserve (Ito et al., 2003) and autoregulatory efficiency (Nur et al., 2009), and CVR impairment has been observed in cerebral steno-occlusive vascular diseases (Mandell et al., 2011; Mandell et al., 2008), lacunar infarction (Birns et al., 2009; Mandell et al., 2011), microbleeding (Birns et al., 2009; Conijn et al., 2012) and cognitive decline in aging as well as dementia (Hurford et al., 2014; Kastrup et al., 1998; Kovács et al., 2010; Suri et al., 2014).

BOLD fMRI during carbon-dioxide ($CO_2$)-based vascular challenges is the most common CVR imaging approach (Kassner et al., 2010), and has been extensively cross-validated (Herzig et al., 2008). $CO_2$ is a potent vasodilator, triggering changes in vascular tension through the arterial baroreflex (Ainslie et al., 2008), and the vascular response to $CO_2$ is well established using transcranial Doppler ultrasound of arterial blood flow (Battisti-Charbonney et al., 2011). Typically, CVR is measured as the ratio between changes in the BOLD fMRI signal and endtidal $CO_2$ ($PETCO_2$) change, a surrogate for arterial $CO_2$ (Robbins et al., 1990).

While the BOLD fMRI method has been the most commonly used due to its high availability and ease of implementation, a well-known concern regarding this approach is that the BOLD signal is not a direct measure of cerebral blood flow (CBF). This concern has been a primary motivation for adopting CBF-based CVR measurement (Noth et al., 2006; Tancredi et al., 2012). While a linear relationship between BOLD- and CBF-based CVR was obtained during hypercapnic vasodilation in healthy controls (Mark et al., 2010) as well as patients (Mandell et al., 2008), these previous experiments imposed iso-oxia during hypercapnic challenges, not the case in the majority of CVR studies. As the BOLD and CBF signals are differentially sensitive to oxygen level changes (Bulte et al., 2007), failure to maintain iso-oxia could introduce biases in the CVR measurements, and the linearity would deteriorate. More importantly, this relationship is still unknown for vasoconstrictive paradigms. In fact, the agreement between BOLD- and CBF-based CVR measurements is potentially dictated by basal vascular tension and type of vascular challenge, as BOLD and CBF signals have differing dependences on baseline blood flow and vascular volume, among other variables (Bhogal et al., 2014).

Commonly, CVR-related vascular changes are induced through manually adjusted administration of blended gasses (Bandettini and Wong, 1997; Cohen et al., 2004; Yezhuvath et al., 2009), endtidal forcing (Poulin et al., 1996) or computerized prospective $PETCO_2$ targeting (Conklin et al., 2011; Han et al., 2011; Mandell et al., 2011; Mandell et al., 2008; Mark et al., 2010; Mikulis et al., 1989; Mutch et al., 2012; Prisman et al., 2008; Slessarev et al., 2007; Spano et al., 2013; Vesely et al., 2001). More recently, breath-holding-based hypercapnia is seen as an increasingly viable alternative (Bright and Murphy, 2013; Murphy et al., 2011). In addition, deep-breathing hypocapnia (Bright et al., 2009; Sousa et al., 2014) has also been proposed as an alternative vascular manipulation. Hypercapnia and hypocapnia result in vasodilation and vasoconstriction, respectively. However, these tasks do

not furnish equivalent CVR measurements, as shown by Tancredi and Hoge (2013). Nonetheless, the relationship between simultaneous BOLD- and CBF-based CVR measurements has yet to be clarified for these widely varying types of vascular manipulations. Such knowledge is particularly useful in the context of altered vascular tension, as BOLD and ASL have diverging dependences on baseline conditions.

Specifically, vascular tension is an important determinant of the degree of vasoconstriction or vasodilation a blood vessel is capable of, and can be altered by age and neuropathology (Lüscher et al., 1991). Thus, understanding the relationship between CVR measurements and vascular tension would help interpret CVR measurements in patients as well as increase CVR data reliability in healthy controls. For instance, in post-stroke individuals, Zhao et al. (2009) reported a significantly lower increase in CBF during hypercapnic challenges but a greater reduction of CBF during hypocapnic challenges than the control group, which may have been attributable to stroke-related long-term alterations in vascular tension. In support of this theory, Ito et al. (2008) reported higher capacity for CBF reduction in a vasodilated state relative to the resting baseline in healthy controls, whereas Bright et al. (2010) identified a reduction in BOLD signal increase during a predilated baseline. The role of baseline vascular tone is more systematically demonstrated by Ghariq et al. (2014), who found that the BOLD $CO_2$ reactivity data fit better to a sigmoidal curve whereas the CBF *versus* $PETCO_2$ data fit better to a linear model. Nonetheless, to the best of our knowledge, there has yet to be a comparison of simultaneously measured BOLD- and CBF-based CVR for various vascular-tension conditions. CVR response delay is also a physiologically meaningful parameter (Blockley et al., 2011; Bright et al., 2010) that may become increasingly useful in assessing vascular dysfunction (Poublanc et al., 2013), but there is also limited information on the dependence of CVR response delay on vascular tension.

In this study, we use a dual-echo pseudocontinuous ASL technique to simultaneously assess the behavior of BOLD- and CBF-based CVR measurements under different vascular tensions and in response to different vascular stimuli. The results demonstrate that BOLD- and CBF-based CVR amplitude measurements are differentially sensitive to vascular tension and to the type of vascular stimuli. Our findings also demonstrate that the $CO_2$ response delay is highly sensitive to baseline vascular tension for both BOLD- and CBF-based CVR measurements. These findings have important implications for comparing BOLD- and CBF-based CVR studies in normal and patient populations.

## Materials and methods

### Participants

This study was carried out with 18 healthy adult volunteers (10 male, age 26.3 ± 6.5 years; range 18 to 36 years). Participants were recruited through the Baycrest Participants Database, which includes participants from Baycrest and the surrounding community. The study was approved by the Baycrest Research Ethics Board.

### MRI acquisition

All images were acquired using a Siemens TIM Trio 3 Tesla System (Siemens, Erlangen, Germany). The scans employed 32-channel phased-array head coil reception and body-coil transmission. A T1-weighted MPRAGE 3D anatomical was acquired at an isotropic resolution of 1 mm. In addition, CBF and BOLD data were acquired concurrently using a dual-echo pseudo-continuous pCASL technique (Dai et al., 2008), with a repetition time (TR) of 4 s, echo times (TE)1/TE2 = 10/25 ms, field of view = 220 × 220 mm, 18 slices (ascending interleaved order), voxel size = 3.4 × 3.4 × 5.0 $mm^3$, 100 frames, bandwidth = 2520 Hz/pixel and GRAPPA = 2. The labeling duration was 1500 ms, and the post-labeling delay was 1000 ms with a mean $G_z$ of 0.6 mT/m which was selected to achieve transit time insensitivity.

### Vascular tension manipulation and vascular challenges

All vascular manipulations were achieved by administering mixtures of $O_2$, $CO_2$ and medical air delivered using the RespirAct™ breathing circuit (Thornhill Research, Toronto, Canada), designed to provide computerized and independent targeting of endtidal $O_2$ ($PETO_2$) and $CO_2$ ($PETCO_2$) pressure using the sequential gas delivery method (Slessarev et al., 2007). This method was chosen to maximize steady-state $PETCO_2$-targeting accuracy and stability while minimizing $PETO_2$ confounds during $CO_2$-based CVR measurements (Chen and Pike, 2010b; Prisman et al., 2008). Within the RespirAct framework, while breath rate was self-regulated, hypocapnia is achieved primarily through increased breathing depths, while hypercapnia is achieved through inhaling air with a higher than normal amount of $CO_2$. For this method, the $CO_2$ and $O_2$ capacity as well as consumption rate for each subject were estimated prior to the scan in order to compensate for the physiology-related resting $PETCO_2$ and $CO_2$ clearance variations between individuals. The detailed experimental protocol is illustrated in Fig. 1.

During the pCASL scans, $PETCO_2$ was sinusoidally modulated (Blockley et al., 2011) at each baseline $PETCO_2$ with a period of 120 s; 3 periods of sinusoidal $PETCO_2$ variations were induced, following a 1-minute baseline. We chose such a bipolar paradigm as it includes both vasodilatory (upper half of sinusoid) and vasoconstrictive (bottom half of sinusoid) components.

This sinusoidal manipulation was applied at the subject's natural baseline (normocapnic) as well as at hypercapnic and hypocapnic baselines, which are both separated from the normocapnic baseline by 4 mm Hg. The ordering of the different baselines was randomized to minimize biases. These mild $PETCO_2$ changes result in slight changes in the subject's vascular tone without noticeable changes in cerebral oxidative metabolism, a potential confound for $CO_2$-based vascular assessment (Chen and Pike, 2010a).

### Image preprocessing

Functional images, including the tag and control images in the pCASL data, and $T_1$-weighted anatomical images were separately preprocessed using SPM8 (Wellcome Trust Centre for Neuroimaging, London, UK). In each of the tag and control series, the first four time frames were discarded to ensure MR steady state. Preprocessing for pCASL images

included retrospective head-motion correction, slice-timing correction using sinc interpolation, spatial transformation into a Montreal Neurological Institute (MNI) space, and spatial smoothing with a 6-mm full-width at half-maximum (FWHM) Gaussian kernel. Anatomical images were co-registered with their corresponding realigned functional data and segmented into gray and white matter tissue probability maps using the unified segmentation procedures (Ashburner and Friston, 2005).

### Data analysis

Analyses were performed using in-house software written in MATLAB (www.mathworks.com) and FSL (www.fmrib.ox.ac.uk/fsl).

### Regions of interest

ROIs were derived from subject-specific native space FreeSurfer tissue parcellations (Fischl et al., 2004) (FreeSurfer software is publically available at http://surfer.nmr.mgh.harvard.edu). Binary masks were also generated for cortical regions, namely the frontal, temporal, parietal, limbic and occipital regions as well as the hippocampus. We also examined subcortical gray matter regions, including the amygdala, caudate, pallidum, putamen and thalamus. Additionally, we created ROIs for global gray matter and white matter. ROIs were then down-sampled to match the resolution of the fMRI data using FreeSurfer.

### BOLD- and CBF-based CVR and CVR-delay calculations

BOLD and CBF time series were generated from the pCASL tag and control images. More specifically, the modulated CBF component, which is less affected by the BOLD-weighted tissue component, was extracted by high-pass filtering the pCASL signal, followed by demodulation, as introduced by Chuang et al. (2008). BOLD contamination in the CBF time series was minimized as described by Tak et al. (2014).

Upon obtaining these time series data, we applied three levels of data control to boost the reliability of the CVR values used in the statistical analysis: (i) control for image-intensity; (ii) control for temporal outliers; and (iii) control for outliers in ROIs.

1. *Control for image intensity values*: Due to the slightly lower signal-to-noise ratio (SNR) of the ASL data in comparison to the BOLD data, we excluded voxels with insufficient SNR by stipulating that at least 60% of the time course has physically positive tag-control difference, given that all data are acquired from healthy adults thus are unlikely to produce negative CBF values. Subsequently, physically negative CBF data was removed and both the CBF and BOLD signals are demeaned to obtain the percent change in the signal relative to the baseline (mean) of the signal.

2. *Control for temporal outliers*: For each voxel, outlier removal was performed by removing points from the time courses that fulfill Student's criterion or a Cook's distance greater than $4/N$, where $N$ is the number of time points. A linear model was applied to regress the $PETCO_2$ time course and the voxel-wise BOLD or CBF time course, and CVR was calculated as the slope of the linear model. The

spatially specific CVR was thresholded at 0 to minimize biases introduced by noise. Additionally, we excluded data associated with any spiking in the $PETCO_2$ time course.

- In calculating CVR, the $CO_2$-response delay in BOLD and CBF time courses were taken into account at each voxel. This delay was estimated from the phase difference between the BOLD or CBF time courses and that of $PETCO_2$, enabling the alignment of the fMRI and $PETCO_2$ time series for maximal correlation. For this alignment, both $PETCO_2$ and fMRI data were upsampled to a common frequency, such that delays that are shorter than TR could be measured. Following the alignment, the $PETCO_2$ was interpolated to the pCASL TR and detrended at half the total duration of the respiratory paradigm.
    - Response to bipolar stimulus: derived by the linear fit of both the upper and lower parts of the MRI signal response to sinusoidal $PETCO_2$ variations;
    - Response to vasodilatory stimulus: derived by the linear fit of the part of the BOLD or CBF signal associated with the upper portion of the $PETCO_2$ sinusoid;
    - Response to vasoconstrictive stimulus: derived by the linear fit of the part of the BOLD or CBF signal associated with the lower portion of the $PETCO_2$ sinusoid;

3 *Control for outliers in ROIs*: We computed the regional mean CVR and standard deviation across each ROI. Specifically, in order to generate representative regional CVR values unbiased by outliers, we first removed outlier voxels from each ROI using the non-parametric algorithm based on the Tukey's box-plot method (Patterson, 2012; Tukey, 1977); this method suits the present application as it does not assume a normal distribution for the voxel-wise CVR values. Subsequently, we performed linear regression to assess the relationship between BOLD- and CBF-based CVR and CVR delay for all ROIs.

## Statistical analysis

The inter-subject mean CBF-derived and BOLD-derived CVR were regressed for the brain lobes and whole brain gray matter (GM) ROIs. Before regression, we implemented the first 2 levels of data control, and removed the outlier data points based on Student's criterion. In addition, we used multi-variate and univariate ANOVA as well as Student's *t*-test to assess the dependence of CVR and CVR-delay values on

- *The level of vascular tension*: modulated through a hypercapnic, normocapnic (resting) and hypocapnic baseline;
- *The type of vascular stimulus*: vasodilatory, vasoconstrictive and bipolar vasodilation–constriction stimulus.

All 3 levels of data control were implemented prior to the ANOVA and *t*-tests.

## Results

The $PETCO_2$ levels corresponding to the three vascular tension levels are shown in Fig. 2a. Prospective targeting permitted us to realize our designated $PETCO_2$ changes, such that the mean $PETCO_2$ was 36.2 ± 1.6, 40.1 ± 1.4 and 44.1 ± 1.5 mm Hg for the hypocapnic, normocapnic and hypercapnic baselines, respectively. The corresponding $PETO_2$ values were 113.5 ± 1.8, 113.0 ± 3.3 and 112.5 ± 4.7 mm Hg, respectively. The sinusoidal $PETCO_2$ modulation (Fig. 2b) induced robust CBF and BOLD signal changes (sample data shown in Fig. 2c).

### Agreement between BOLD- and CBF-based CVR

CVR maps were successfully generated using both BOLD and CBF data, as shown in Fig. 3, with BOLD maps exhibiting superior signal-to-noise (SNR) than CBF. BOLD- and CBF-based CVR measurements were significantly correlated in the majority of brain regions. This was true for the CVR amplitude (Fig. 4) as well as response delay (Fig. 5). In spite of the existence of linear relationships between BOLD and CBF-based CVR measurements, these measurements have different sensitivities to vascular tone and to the nature of the vascular stimulus.

### The effect of vascular stimulus type on CVR measurement

At normocapnic (resting) vascular tension, after performing all 3 levels of data control, we found the group-average BOLD CVR to be 0.05 ± 0.005% BOLD/mm Hg in the cortex and 0.03 ± 0.002% BOLD/mm Hg in the white matter, taken across all participants. In the case of CBF-based CVR, the cortical and white matter group averages were 1.9 ± 0.4 and 1.1 ± 0.3% CBF/mm Hg, respectively. With regards to the effect of the choice of vascular stimulus, the results are illustrated in Fig. 6, and the ANOVA assessments in Table 1. When all vascular tension levels were considered, we found no significant distinction in the BOLD-based measurements, *i.e.* BOLD CVR = 0.04 ± 0.007, 0.03 ± 0.007 and 0.05 ± 0.008% BOLD/mm Hg, respectively, as the cortical average for vasodilatory, vasoconstrictive and bipolar stimuli. However, for CBF, the vasodilatory stimulus to elicit higher responses was comparable to vasoconstrictive and bipolar stimuli in multiple brain regions, including the frontal, limbic and occipital lobes as well as the amygdala and hippocampus ($p < 0.05$).

### The effect of baseline vascular tension on CVR measurement

The effect of vascular tension on CRV estimation is also summarized in Table 1. When considering both vasodilatory and vasoconstricting stimuli (Fig. 7), we found that BOLD-based CVR was highest during hypercapnic (predilated) baseline, followed by hypocapnic (preconstricted) baseline, with normocapnic (resting) baseline being associated with the lowest CVR values. Similar trends were also observed for CBF CVR measurements throughout the cortex and deep-gray structures. The white matter did not show a significant vascular-tension effect.

We illustrate the dependence of the vasodilatory response to vascular tension in Fig. 8. In regard to BOLD CVR, we found that a normocapnic baseline was associated with the

highest vasodilatory response, with both predilation (hypercapnic baseline) and preconstriction (hypocapnic baseline) both leading to a lower vasodilatory CVR. This was a significant effect in the temporal lobe and thalamus. In contrast, CBF-based vasodilatory CVR measurements were, highest in the predilated and resting baselines (at similar levels), and lowest in the preconstricted state. This effect was significant in the parietal lobe alone.

The influence of vascular tension on the vasoconstrictive stimulus is illustrated in Fig. 9. The predilated state was associated with higher BOLD and CBF responses than resting and preconstricted baselines. These effects were dominant in the cortex (frontal, temporal and occipital regions) and not significant in the subcortical regions. Once again, CBF-based CVR measurements exhibited less vascular-tension dependence than BOLD-based CVR.

### The effect of baseline vascular tension on $CO_2$ response delay

Finally, the impact of basal vascular tension on the $CO_2$ response delays is summarized in Fig. 10 and Table 2. We opted to use the response to the bipolar stimulus alone in order to maximize the accuracy of delay estimation. Across all baseline conditions, we found BOLD-based CVR delay to be 10.4 ± 1.4 s for the frontal lobe, 10.8 ± 1.2 s for the parietal lobe, 10.9 ± 1.2 s for the temporal lobe, 9.9 ± 1.1 s for the limbic lobe, 11.0 ± 1.1 s for the occipital lobe and 11.7 ± 1.2 s for the thalamus. A similar regional variation was seen in the CBF-based estimate, although more pronounced. The average BOLD-based CVR delay was 10.2 ± 1.1 s in the cortex and 10.6 ± 1.2 s in the white matter, longer than the average CBF-based cortical and white-matter delays of 9.2 ± 1.7 s and 9.5 ± 1.9 s, respectively. During the predilated baseline, these delays increased significantly relative to the resting baseline, by as much as 8.2 s across all brain regions. In fact, we found that the $CO_2$ response delay was the largest at the predilated baseline, while the difference between preconstricted and resting baselines was not statistically significant; this was true for both BOLD and CBF.

## Discussion

In this work, we used simultaneous BOLD-CBF measurements during vasodilatory and vasoconstrictive tasks to measure CVR. These tasks were in the form of $PETCO_2$ manipulations, well known for inducing robust intravascular $CO_2$ and blood-flow changes. We further imposed three levels of baseline vascular tension to emulate arterial pressure changes characteristic of normal vascular variability and potential disease conditions. In each individual, we modulated vascular tension through different capnic states, focusing on mild vascular-tension changes so as to avoid inducing non-vascular confounds. Even within this small range of variations, we saw significant and diverse dependencies in both the BOLD and CBF measurements of CVR. These findings are expected to be important considerations when interpreting CVR measurements.

### The effect of vascular stimulus type on CVR measurement

The first main message of this work is that CBF-based CVR measurements are far more sensitive to the type of vascular stimulus than BOLD-based CVR, with higher CVR during vasodilatory tasks. Indeed, when comparing BOLD-based CVR measurements made using breath-holding hypercapnia and deep-breathing hypocapnia, Bright et al. (2009) noted that

vasoconstrictive responses are generally lower than vasodilatory responses. A similar trend was described by Tancredi and Hoge (2013), with hyperventilation-induced hypocapnia resulting in lower CBF responses than either breathholding or prospectively-targeted hypercapnia. Such observations are consistent with the sigmoidal model of the dependence of blood flow on $CO_2$ (Battisti-Charbonney et al., 2011; Claassen et al., 2007; Tancredi and Hoge, 2013), derived based on transcranial Doppler data from healthy adults, describing diminished arterial blood-flow response sensitivity to $CO_2$ below and above a certain $PETCO_2$ range. This model was recently validated by Sobczyk et al. (2014) using BOLD data. We attribute the lack of similar effects in our BOLD data to our particular vascular tasks, which induce much smaller $PETCO_2$ changes than expected from previous studies. Surprisingly however, the bipolar stimulus elicited lower CBF CVR than either the vasodilatory or the vasoconstrictive stimulus. This was a robust finding in all brain regions examined, and indicates that CBF CVR values obtained from different stimulus types should not be compared. This finding could be explained by the lower CBF vasoconstrictive reactivity compared to the vasodilatory reactivity, potentially due to SNR limitations in ASL data in low-flow conditions. Such an experimental limitation would potentially result in a non-linear CBF dependence on $PETCO_2$ from low to high values, and fitting a linear model to such data would result in a shallower slope than fitting to the upper or lower half alone.

### The effect of baseline vascular tension on CVR measurement

The second main message of this paper is that it is important to be aware of heterogeneity in basal vascular tension when comparing CVR measurements across individuals. Given the disparities in the dependence of the BOLD and CBF signals on vascular baseline, vascular tension is key to the interpretation of MRI-based CVR measurements.

When using the bipolar stimulus, the BOLD CVR values were generally lower at the preconstricted (hypocapnic) baseline (Figs. 7a). A similar trend was also observed in the CBF data. This is in fact also consistent with predictions of the sigmoidal model, describing diminished arterial blood-flow response sensitivity to $CO_2$ below and above a certain $PETCO_2$ range. Vascular tension reflects arterial pressure, and both the predilated and preconstricted baselines are associated with elevated arterial blood pressure (Carrera et al., 2009). These in turn modulate the ability of a blood vessel to dilate and contract passively by the change in arterial blood pressure. Using transcranial Doppler ultrasound, Carrera et al. (2009) found CVR to be reduced in the presence of increased arterial pressure, being significantly higher in a mildly hypocapnic state. Furthermore, our findings agree with those of Tancredi and Hoge, showing that even moderately hypocapnic baseline can bring CBF-CVR into the non-linear $CO_2$ response regime, resulting in significantly diminished CVR compared to normocapnic and mildly hypercapnic conditions.

In practice, most existing CVR studies have not used bipolar stimuli, but rather vasodilatory stimuli alone (Kassner et al., 2010; Mandell et al., 2011; Mandell et al., 2008; Mark et al., 2010). Our finding of the vascular-tension dependence of BOLD and CBF vasodilatory CVR is relevant to the majority of CVR results. The higher BOLD dilatory response in the resting baseline compared to at the predilated baseline is in agreement with findings by Bright et al. (2010), and is potentially attributable to altered vascular compliance with arterial pressure

changes. We note that our finding of a higher BOLD-CVR at normocapnia than at hypercapnia differs from the pattern observed in CBF-CVR estimates. This may be a reflection of the physical differences in the origins of the BOLD and CBF signals, implying that BOLD- and CBF-CVR likely do not share the same linear and non-linear regimes, as will be discussed in a later section. Interestingly, within the range of $PETCO_2$ values used in our study, the CBF dilatory response was slightly less affected by vascular tension, suggesting that CBF CVR measurements are potentially more robust than BOLD.

There is an increasing interest to use hypocapnia for CVR measurement, particularly as the recently proposed cued deep-breathing paradigm is more patient-friendly than existing hypercapnia paradigms (Bright et al., 2009; Sousa et al., 2014). In this regard, a significant trend towards higher vasoconstrictive BOLD CVR at the predilated baseline was observed. A similar but less significant trend was observed in CBF measurements. Such trends support previous findings (Bright et al., 2010; Ito et al., 2008). Ito et al. used a spectrum of intrinsic variations in resting CBF to investigate the dependence of CBF response on vascular baseline, and found that in most brain regions, a higher basal CBF was associated with a higher vasoconstriction capacity and a lower vasodilatory capacity. Similar findings were reported by Liu et al. (2012) in large cerebral arteries.

The sensitivity of CBF CVR to vascular tension is lower but in keeping with findings by Ito et al. We note, nonetheless, that Ito et al. reported considerable spatial dependence in this relationship, and in fact, the frontal and occipital lobes seemed to show opposite trends. We noted a substantial degree of regional heterogeneity in the trends observed in our data as well, which may obscure the global trend. We also note that in our study, instead of relying on cross-sectional basal CBF differences, we modulated basal vascular tension in each individual through computerized $CO_2$ targeting. We argue that our approach minimizes the confounding influence of potential neurovascular properties (such as CVR itself) that may have led to these inter-subject CBF differences in the first place. These methodological differences may help to explain some of the differences across studies. Last but not least, the insensitivity of dilatory CBF reactivity to vascular tension may also be attributed to the lower SNR in the CBF data. Paradoxically, in our data, the hypocapnic baseline did not result in a higher vasodilatory BOLD reactivity compared to the normocapnic baseline. As described earlier, such behavior may indicate that the arterial blood pressure increase associated with our hypocapnic baseline condition has begun to compromise arterial compliance.

### The effect of baseline vascular tension on $CO_2$ response delay

In this work, we used the sinusoidal stimulus proposed by Blockley et al. (2011). However, we did not use the frequency spectrum-based technique for response delay estimation, as low-frequency physiological noise interfered within the frequency bandwidth of our stimulus. Rather, our delay-estimation method is similar to that of Thomas et al. (2014). Nonetheless, our findings of earlier response in the frontal lobe and later response in the occipital lobe as well as the subcortical gray matter structures are in agreement with previous findings (Blockley et al., 2011; Bright et al., 2009). We do not quantitatively

compare our delay estimates with those of Blockley et al. as the latter results were obtained at 7 T.

Our third major finding in this work is that vascular response delay is longest at a predilated vascular baseline. We observed the longest delay at the hypercapnic baseline in both BOLD and CBF data. As the CVR response to the vasodilatory stimulus is generally higher, the delay estimates may have been dominated by the vasodilatory response, and thus show the $CO_2$ response to be more sluggish when the vessels are predilated. Such a finding could be evidence of the behavior described by the arteriolar-compliance model (Behzadi and Liu, 2005), which predicts that the baseline vascular state would affect CVR by changing the relative contributions of an active smooth muscle component and a passive connective tissue component to the overall vascular reactivity. According to this model, one would expect the vascular response to any vasoactive agent to be slower in a predilated state, as the slower passive-tissue component dominates at larger vascular radii. A potential alternative explanation is that as basal vascular diameter increases, more incoming blood is required to achieve a certain fractional vascular signal increase, resulting in the appearance of an increasing BOLD and CBF CVR delay. However, a contradicting observation to both theories is that the preconstricted baseline did not result in a significant reduction in CVR delay. Further investigation is necessary to clarify the nature of our observation.

### Basal vascular tension variations in health and disease

In the absence of external stimuli, CBF stays constant over a range of mean arterial pressure (MAP) values as part of cerebral autoregulation (Paulson et al., 1990). However, vascular diameter and vascular tension can be modulated in a dose-dependent fashion by vasoactive agents such as caffeine (Rack-Gomer and Liu, 2012). Moreover, the arterial $CO_2$ fluctuations introduced in this study are a part of normal daily activities, resulting in a major source of vascular tension changes. According to the detailed characterization by Battisti-Charbonney et al., the linear regime for vasodilation-mediated blood flow velocity response to $CO_2$ in a healthy adult can span no more than 4 mm Hg above and below normocapnia, beyond which MAP will no longer remain unchanged. Thus, as our multi-baseline and sinusoidal stimulation approach probes $PETCO_2$ values up to 8 mm Hg above and below normal baseline, we involve both the constant-MAP and variable-MAP regimes of CBF regulation. As shown by Carrera et al., a $\Delta PETCO_2$ of 8 mm Hg could induce a MAP increase of up to 10%, whether for hypercapnia or hypocapnia. A similar degree of MAP reduction can result from less than 30 min of physical exercise (Pescatello et al., 1991; Sun et al., 2014).

More importantly, vascular tension is a common indicator of vascular health. Hypertension entails increased MAP, reduced vascular compliance, and is widely identified with atherosclerosis, diabetes, heart disease and obesity (Benetos, 2008; van Popele et al., 2001). In diabetes mellitus, for instance, MAP is on average 10% higher than in age-matched controls, whereas in clinically hypertensive patients, MAP can measure up to 40% higher (Megnien et al., 1992). The hypertension and vascular lumen narrowing seen in atherosclerosis can be simulated by our hypocapnic baseline in terms of the hypoperfusion and reduced vasoconstrictive compliance, with the complication that vasodilatory response

is also compromised due to vascular stiffening in atherosclerosis (van Popele et al., 2001). On the other hand, cerebral hyperperfusion syndrome, which has been associated with seizures (Ho et al., 2000), is analogous to our hypercapnic baseline. Even healthy aging, older adults have been associated with an average MAP of up to 4% higher than middle-aged adults (Sesso et al., 2000).

### BOLD-based vs. CBF-based CVR

We note that after ROI-wise outlier removal, our mean BOLD-based CVR values reported here became much lower than those found in the literature (*e.g.* cortical mean CVR reduced from 0.13 to 0.05% BOLD/mm Hg at normocapnia). For instance, using various hypercapnic manipulations, Stefanovic et al. (2006) (1.5 T), Yezhuvath et al. (2009) (3 T), Kassner et al. (2010) (1.5 T) and Mark et al. (2010) (3 T) listed BOLD CVR values of 0.1–0.2% BOLD/mm Hg, while Bright et al. (2009) reported values up to 0.5%/mm Hg using hypocapnia. We note that Kassner et al. reported a mean normocapnic cortical BOLD CVR of 0.14%/mm Hg using a precise $PETCO_2$ targeting paradigm very similar to our own, but upon closer inspection, the CVR maps shown by Kassner et al. seem to reflect parenchymal CVR values much lower, primarily between 0.01 and 0.025%/mm Hg (at 1.5 T). Similarly low values were shown by Vesely et al. (2001), more akin to our own findings of mean CVRs of 0.05% BOLD/mm Hg at 3 T. The most logical explanation is that the reported high mean-CVR values were driven by large vessel effects in BOLD, which we were able to suppress through our ROI-wise outlier exclusion strategy. Thus, our measurements rather reflect the parenchymal contribution to the BOLD CVR measurements. Incidentally, CBF-based CVR values did not seem to be as sensitive to the ROI-wise outlier exclusion, suggesting that CBF-based measurements are less prone to large-vessel effects, as they were less weighed towards veins. This is an important distinction between BOLD and CBF that will likely become critical in distinguishing parenchymal and vascular health.

By nature, CBF measured using ASL takes into account both vasodilatory CBF and velocity-driven CBF increases. This is not the case with BOLD. Based on the BOLD signal model (Davis et al., 1998; Hoge et al., 1999), the BOLD signal increases due to the dilution of deoxyhemoglobin by CBF increases. Thus, when deoxyhemoglobin dilution reaches a maximum, further increases in CBF would not be reflected in the BOLD signal. Conversely, when the lowest deoxyhemoglobin-concentration steady state has been reached, no further reductions in CBF would be reflected in BOLD. These scenarios were compellingly illustrated by Sobczyk et al. (2014) in patients with steno-occlusive disease. Both of these states would entail MAP changes (see earlier discussion), to which BOLD is theoretically insensitive. Thus, analogous to the case presented by Regan et al. (2014), BOLD is likely to underestimate CVR when MAP is not constant. We simulated these situations using the vasoconstrictive stimulus in the hypocapnic baseline as well as vasodilatory stimulus in hypercapnic baseline, and indeed observed such an effect, as illustrated in Fig. 11. BOLD-based CVR to the vasodilatory stimulus was lower at hypercapnic baseline compared to normocapnic baseline, but CBF maintained a larger linear range with increasing $PETCO_2$, consistent with ultrasound recordings (Battisti-Charbonney et al., 2011). However, we did observe a trend of lower CBF response to vasoconstrictive than to vasodilatory stimulus, consistent with previous MRI findings (Tancredi and Hoge, 2013). We attribute this

primarily to potential transit-time effects in the ASL technique, and secondarily to SNR limitations in low-flow conditions. Potential remedies include novel techniques such as velocity-selective ASL (Wu and Wong, 2006).

### Recommendations and significance

First, as the dependence of CVR measurements on baseline vascular tension becomes an important consideration when $PETCO_2$ enters the non-linear regime (Battisti-Charbonney et al., 2011), our results reinforce support for the recommendation by Tancredi and Hoge that CVR studies should be conducted within the linear range of $PETCO_2$ dependence, which is above 30 and below 45 mm Hg (Battisti-Charbonney et al., 2011; Tancredi and Hoge, 2013). However, even with the small range of $PETCO_2$ variations used in our study, we still observed vascular-tension dependence in the BOLD CVR measurements. On that note, BOLD and CBF, due to their fundamental differences in signal origin, are associated with different linear and non-linear $PETCO_2$ regimes. In fact, as shown very recently by Ghariq et al. (2014), the linear regime of the CBF CVR measurements may be more extensive than that of BOLD, which was demonstrated as not being solely driven by the differential SNR between BOLD and CBF. Thus, our results support the view that CBF may provide somewhat less biased CVR measurements than BOLD.

Secondly, vasodilatory and vasoconstrictive stimuli exhibited similar sensitivities to basal vascular tension. Bipolar stimuli, such as the sinusoidal paradigm used here, were also affected by vascular tension, but to a greater extent than either of the other two paradigms. Furthermore, CBF-based CVR measurements obtained using a bipolar stimulus were the most sensitive to vascular tension, and may be the best choice when sensitivity is desired. However, CBF-based CVR to the vasodilatory stimulus is the least affected by vascular tension, and may be a good choice when tension information was unavailable. Finally, in view of these dependencies, we recommend that MAP measurements be incorporated into future CVR studies to provide a means to account for biases.

The above findings relate to a healthy vasculature among relatively young adults, in whom control of $CO_2$-elicited vascular response has not been impaired. This may not always be the case in CVR studies. For example, aging is associated with increasing blood pressure (potentially diminished ability to vasodilate further) despite decreasing CBF, as well as increasing vascular stiffness (Tarumi et al., 2014). CVR reduction in the elderly may therefore be exaggerated, as this reduction may be due both to increased vascular stiffness and to the lengthened vascular response delay in a vasodilated state. In addition, CVR impairment as reflected by a comparison of vasodilatory and vasoconstrictive responses may help to dissect the effects of blood pressure increase and vascular stiffness.

While vascular stiffness is also associated with diabetes (van Elderen et al., 2011) and cognitive impairment (Scuteri et al., 2005), current clinical applications of CVR measurements have mostly been found in the study of stroke (Zhao et al., 2009) and occlusive diseases. Notably, regional vasodilation is characteristic of carotid occlusion (Kavec et al., 2004), which could be in part emulated by our predilated vascular baseline. An observation of enhanced vasoconstrictive and diminished vasodilatory response in such

patients in spite of compromised vasodilatory response may suggest that CVR is not truly impaired.

## Potential caveats

When comparing our work with previous studies, we have found disparities potentially attributable to the definition of “hypercapnia” and “hypocapnia”. As we noted earlier, vascular response becomes diminished when vascular tension encroaches on the non-linear $PETCO_2$-response range. However, in view of the diverse implementations of hyper- and hypocapnia in the literature, it is difficult to closely compare results from different studies. For instance, most relevant studies have used the breathing of carbogen–air mixtures to achieve different capnic conditions (Bright et al., 2010; Ito et al., 2008), with no control of the actual $PETCO_2$ levels achieved or minimization of concurrent endtidal oxygen changes. Conversely, in our methodology, we strictly controlled $PETCO_2$ to vary within a ±4 mm Hg range. In addition, we constrained our $CO_2$ manipulations to lower levels than were used in previous studies, and minimized concurrent changes in endtidal pressure of oxygen, which has been known to modulate BOLD and CBF signals, though mildly in comparison with $CO_2$ (Bulte et al., 2007; Prisman et al., 2008).

We recognize that in minimizing metabolic confounds with our moderate hypercapnic and hypocapnic manipulations, we may be limited in our ability to truly simulate disease conditions, which typically entail much greater changes in MAP (see earlier Discussion). We also recognize that higher capnic challenges than ours have been commonly used in CVR studies employing prospective targeting, involving $\Delta PETCO_2$ of up to 10 mm Hg above baseline (Kassner et al., 2010; Mandell et al., 2011; Sobczyk et al., 2014; Tancredi and Hoge, 2013). However, given our knowledge of known limitations of BOLD fMRI, we feel the need to adhere to such a limited range. We feel nonetheless that our conceptual demonstration of potential biases in CVR measurement in this limited range offers valid insight into measurement biases associated with disease conditions. Our future work will be directed towards the use of more advanced imaging techniques to probe higher MAP ranges.

Finally, a well known confound of a study such as ours is the low SNR of ASL data. Such concerns were noted earlier with regards to the ability of ASL to capture CBF changes in low-flow conditions, *i.e.* at a hypocapnic baseline. In this work, typical temporal SNR (mean effect size/stdev, bipolar stimulus) for the BOLD signal is ~7.0 for gray matter and 3.0 for white matter. For CBF data, the SNR is 3.5 and 1.5, respectively. Moreover, we noted that more voxels in the white matter were associated with negative, noise-driven CBF-CVR estimates, and these were excluded from our analyses. However, as Ghariq et al. (2014) demonstrated, a linear relationship better explains the variation of CBF-CVR with basal $PETCO_2$ than a nonlinear one, even when accounting for the lower CBF SNR. Despite our conclusion of higher robustness of CBF CVR measurements against vascular tone and type of vascular stimuli, the use of ASL for CVR measurement would perhaps be difficult if voxel-wise comparisons are desired, and may need to be based on satisfactory power analysis to ensure that the effects of interest would be captured in spite of the lower SNR.

## Conclusion

Accurate and reproducible CVR mapping tools have important implications for studying cerebrovascular health. In this study, we provide empirical evidence that while BOLD-derived CVR and CBF-derived CVR are significantly correlated in most regions, they do not behave in the same manner under altered vascular tension. This finding is potentially attributable to the different physical origins of the BOLD and CBF signals. In addition, this vascular-tension dependence differs between vasodilatory and vasoconstrictive responses, necessitating caution in the choice of vascular paradigm and when comparing across studies. Finally, we explore the dependence of CVR response delay on vascular tension, and find predilation to lead to slower $CO_2$ reactivity. Thus, this study addresses differences between vascular stimuli, different vascular tension levels and the choice of BOLD *vs.* CBF when measuring CVR, and is directly relevant to CVR-based imaging research into cerebrovascular health.

## Acknowledgments

We are grateful to Drs. Danny J. Wang and Lirong Yan from the University of California at Los Angeles for providing the dual-echo pCASL sequence, and to Dr. Joseph Fisher and Ms. Olivia Sobczyk (University of Toronto) for assistance with the respiratory task setup. We also thank Mr. Mohsin Kazmi for assisting with data collection. This research was supported by the Natural Sciences and Engineering Council of Canada, the Canadian Institutes of Health Research and the Heart and Stroke Foundation Centre for Stroke Recovery (J. B. Kwinta).

## References

Ainslie PN, Celi L, McGrattan K, Peebles K, Ogoh S. Dynamic cerebral autoregulation and baroreflex sensitivity during modest and severe step changes in arterial $PCO_2$. Brain Res Rev. 2008; 230:115–124.

Bandettini PA, Wong EC. A hypercapnia-based normalization method for improved spatial localization of human brain activation with fMRI. NMR Biomed. 1997; 10:197–203. [PubMed: 9430348]

Battisti-Charbonney A, Fisher J, Duffin J. The cerebrovascular response to carbon dioxide in humans. J Physiol. 2011; 589:3039–3048. [PubMed: 21521758]

Behzadi Y, Liu TT. An arteriolar compliance model of the cerebral blood flow response to neural stimulus. NeuroImage. 2005; 25:1100–1111. [PubMed: 15850728]

Benetos A. Arterial stiffness and systolic hypertension: determinants, assessment, and clinical consequences. Curr Cardiovasc Risk Rep. 2008; 2:410–415.

Bhogal AA, Siero JCW, Fisher JA, Froeling M, Luijten P, Philippens M, Hoogduin H. Investigating the non-linearity of the BOLD cerebrovascular reactivity response to targeted hypo/hypercapnia at 7 T. NeuroImage. 2014; 98:296–305. [PubMed: 24830840]

Birns J, Jarosz J, Markus HS, Kalra L. Cerebrovascular reactivity and dynamic autoregulation in ischaemic subcortical white matter disease. J Neurol Neurosurg Psychiatry. 2009; 80:1093–1098. [PubMed: 19535355]

Blockley NP, Driver ID, Francis ST, Fisher JA, Gowland PA. An improved method for acquiring cerebrovascular reactivity maps. Magn Reson Med. 2011; 65:1278–1286. [PubMed: 21500256]

Bright MG, Murphy K. Reliable quantification of BOLD fMRI cerebrovascular reactivity despite poor breath-hold performance. NeuroImage. 2013; 83:559–568. [PubMed: 23845426]

Bright MG, Bulte DP, Jezzard P, Duyn JH. Characterization of regional heterogeneity in cerebrovascular reactivity dynamics using novel hypocapnia task and BOLD fMRI. NeuroImage. 2009; 48:166–175. [PubMed: 19450694]

Bright MG, Donahue MJ, Duyn JH, Jezzard P, Bulte DP. The effect of basal vasodilation on hypercapnic and hypocapnic reactivity measured using magnetic resonance imaging. J Cereb Blood Flow Metab. 2010; 31:426–438. [PubMed: 20959855]

Bulte DP, Chiarelli PA, Wise RG, Jezzard P. Cerebral perfusion response to hyperoxia. J Cereb Blood Flow Metab. 2007; 27:69–75. [PubMed: 16670698]

Carrera, E., Kim, DJ., Castellani, G., Zweifel, C., Smielewski, P., Pickard, JD., Czosnyka, M. Effect of hyper- and hypocapnia on cerebral arterial compliance in normal subjects. J Neuroimaging. 2009. http://dx.doi.org/10.1111/j.1552-6569.2009.00439.x

Chen JJ, Pike GB. Global cerebral oxidative metabolism during hypercapnia and hypocapnia in humans: implications for BOLD fMRI. J Cereb Blood Flow Metab. 2010a; 30:1094–1099. [PubMed: 20372169]

Chen JJ, Pike GB. MRI measurement of the BOLD-specific flow–volume relationship during hypercapnia and hypocapnia in humans. NeuroImage. 2010b; 53:383–391. [PubMed: 20624474]

Chuang KH, Gelderen PV, Merkle H, Bodurka J, Ikonomidou VN, Koretsky AP, Duyn JH, Talagala SL. Mapping resting-state functional connectivity using perfusion MRI. NeuroImage. 2008; 40:1595–1605. [PubMed: 18314354]

Claassen JAHR, Zhang R, Fu Q, Witkowski S, Levine BD. Transcranial Doppler estimation of cerebral blood flow and cerebrovascular conductance during modified rebreathing. J Appl Physiol. 2007; 102:870–877. [PubMed: 17110510]

Cohen ER, Rostrup E, Sidaros K, Lund TE, Paulson OB, Ugurbil K, Kim SG. Hypercapnic normalization of BOLD fMRI: comparison across field strengths and pulse sequences. NeuroImage. 2004; 23:613–624. [PubMed: 15488411]

Conijn MM, Hoogduin JM, van der Graaf Y, Hendrikse J, Luijten PR, Geerlings MI. Microbleeds, lacunar infarcts, white matter lesions and cerebrovascular reactivity — a 7 T study. NeuroImage. 2012; 59:950–956. [PubMed: 21930217]

Conklin J, Fierstra J, Crawley AP, Han JS, Poublanc J, Silver FL, Tymianski M, Fisher JA, Mandell DM, Mikulis DJ. Mapping white matter diffusion and cerebrovascular reactivity in carotid occlusive disease. Neurology. 2011; 77:431–438. [PubMed: 21775744]

Dai W, Garcia D, De Bazelaire C, Alsop DC. Continuous flow-driven inversion for arterial spin labeling using pulsed radio frequency and gradient fields. Magn Reson Med. 2008; 60:1488–1497. [PubMed: 19025913]

Davis TL, Kwong KK, Weisskoff RM, Rosen BR. Calibrated functional MRI: mapping the dynamics of oxidative metabolism. Proc Natl Acad Sci U S A. 1998; 95:1834–1839. [PubMed: 9465103]

Fischl B, van der Kouwe A, Destrieux C, Halgren E, Segonne F, Salat DH, Busa E, Seidman LJ, Goldstein J, Kennedy D, Caviness V, Makris N, Rosen B, Dale AM. Automatically parcellating the human cerebral cortex. Cereb Cortex. 2004; 14:11–22. [PubMed: 14654453]

Ghariq, E., Zhang, X., Webb, AG., van Buchem, MA., Dahan, A., van Osch, MJ. Int Soc Magn Reson Med, Milan. 2014. The dependency of cerebral blood flow on endtidal $CO_2$ pressure; p. 213

Han JS, Abou-Hamden A, Mandell DM, Poublanc J, Crawley AP, Fisher JA, Mikulis DJ, Tymianski M. Impact of extracranial–intracranial bypass on cerebrovascular reactivity and clinical outcome in patients with symptomatic moyamoya vasculopathy. Stroke. 2011; 42:3047–3054. [PubMed: 21903951]

Herzig R, Hlustík P, Skoloudík D, Sanák D, Vlachová I, Herman M, Kanovský P. Assessment of the cerebral vasomotor reactivity in internal carotid artery occlusion using a transcranial Doppler sonography and functional MRI. J Neuroimaging. 2008; 18:38–45. [PubMed: 18190494]

Ho DS, Wang Y, Chui M, Ho SL, Cheung RT. Epileptic seizures attributed to cerebral hyperperfusion after percutaneous transluminal angioplasty and stenting of the internal carotid artery. Cerebrovasc Dis. 2000; 10:374–379. [PubMed: 10971023]

Hoge RD, Atkinson J, Gill B, Crelier GR, Marrett S, Pike GB. Investigation of BOLD signal dependence on cerebral blood flow and oxygen consumption: the deoxyhemoglobin dilution model. Magn Reson Med. 1999; 42:849–863. [PubMed: 10542343]

Hurford R, Charidimou A, Fox Z, Cipolotti L, Jager R, Werring DJ. MRI-visible perivascular spaces: relationship to cognition and small vessel disease MRI markers in ischaemic stroke and TIA. J Neurol Neurosurg Psychiatry. 2014; 85:522–525. [PubMed: 24249785]

Ito H, Kanno I, Ibaraki M, Hatazawa J, Miura S. Changes in human cerebral blood flow and cerebral blood volume during hypercapnia and hypocapnia measured by positron emission tomography. J Cereb Blood Flow Metab. 2003; 23:665–670. [PubMed: 12796714]

Ito H, Kanno I, Ibaraki M, Suhara T, Miura H. Relationship between baseline cerebral blood flow and vascular responses to changes in $PaCO_2$ measured by positron emission tomography in humans: implication of inter-individual variations of cerebral vascular tone. Acta Physiol. 2008; 193:325–330.

Kassner A, Winter JD, Poublanc J, Mikulis DJ, Crawley AP. Blood-oxygen level dependent MRI measures of cerebrovascular reactivity using a controlled respiratory challenge: reproducibility and gender differences. J Magn Reson Imaging. 2010; 31:298–304. [PubMed: 20099341]

Kastrup A, Dichgans J, Niemeier M, Schabet M. Changes of cerebrovascular $CO_2$ reactivity during normal aging. Stroke. 1998; 29:1311–1314. [PubMed: 9660378]

Kavec M, Usenius JP, Tuunanen PI, Rissanen A, Kauppinen RA. Assessment of cerebral hemodynamics and oxygen extraction using dynamic susceptibility contrast and spin echo blood oxygenation level-dependent magnetic resonance imaging: applications to carotid stenosis patients. NeuroImage. 2004; 22:258–267. [PubMed: 15110016]

Kovács KR, Szekeres CC, Bajkó Z, Csapó K, Molnár S, Olah L, Csiba L. Cerebro-and cardiovascular reactivity and neuropsychological performance in hypertensive patients. J Neurol Sci. 2010; 299:120–125. [PubMed: 20800240]

Liu YJ, Huang TY, Lee YH, Juan CJ. The cerebral vasomotor response in varying $CO_2$ concentrations, as evaluated using cine phase contrast MRI: flow, volume, and cerebrovascular resistance indices. Med Phys. 2012; 39:6534–6541. [PubMed: 23127048]

Lüscher TF, Dohi Y, Tanner FC, Boulanger C. Endothelium-dependent control of vascular tone: effects of age, hypertension and lipids. Basic Res Cardiol. 1991:86.

Mandell DM, Han JS, Poublanc J, Crawley AP, Stainsby JA, Fisher JA, Mikulis DJ. Mapping cerebrovascular reactivity using blood oxygen level-dependent MRI in patients with arterial steno-occlusive disease: comparison with arterial spin labeling MRI. Stroke. 2008; 39:2021–2028. [PubMed: 18451352]

Mandell DM, Han JS, Poublanc J, Crawley AP, Fierstra J, Tymianski M, Fisher JA, Mikulis DJ. Quantitative measurement of cerebrovascular reactivity by blood oxygen level-dependent MR imaging in patients with intracranial stenosis: preoperative cerebrovascular reactivity predicts the effect of extracranial–intracranial bypass surgery. AJNR Am J Neuroradiol. 2011; 32:721–727. [PubMed: 21436343]

Mark CI, Slessarev M, Ito S, Han J, Fisher JA, Pike GB. Precise control of endtidal carbon dioxide and oxygen improves BOLD and ASL cerebrovascular reactivity measures. Magn Reson Med. 2010; 64:749–756. [PubMed: 20648687]

Megnien JL, Simon A, Valensi P, Flaud P, Merli I, Levenson J. Comparative effects of diabetes mellitus and hypertension on physical properties of human large arteries. J Am Coll Cardiol. 1992; 20:1562–1568. [PubMed: 1452931]

Mikulis DJ, Chisin R, Wismer GL, Buxton RB, Weber AL, Davis KR, Rosen B. Phase-contrast imaging of the parotid region. AJNR Am J Neuroradiol. 1989; 10:157–164. [PubMed: 2492717]

Murphy K, Harris AD, Wise RG. Robustly measuring vascular reactivity differences with breath-hold: normalizing stimulus-evoked and resting state BOLD fMRI data. NeuroImage. 2011; 54:369–379. [PubMed: 20682354]

Mutch WAC, Mandell DM, Fisher JA, Mikulis DJ, Crawley AP, Pucci O, Duffin J. Approaches to brain stress testing: BOLD magnetic resonance imaging with computer-controlled delivery of carbon dioxide. PLoS ONE. 2012; 7:e47443. [PubMed: 23139743]

Noth U, Meadows GE, Kotajima F, Deichmann R, Corfield DR, Turner R. Cerebral vascular response to hypercapnia: determination with perfusion MRI at 1.5 and 3.0 Tesla using a pulsed arterial spin labeling technique. J Magn Reson Imaging. 2006; 24:1229–1235. [PubMed: 17094105]

Nur E, Kim YS, Truijen J, van Beers EJ, Davis SC, Brandjes DP, Biemond BJ, van Lieshout JJ. Cerebrovascular reserve capacity is impaired in patients with sickle cell disease. Blood. 2009; 114:3473–3478. [PubMed: 19700663]

Patterson, N. A robust, non-parametric method to identify outliers and improve final yield and quality. CS MANTECH; Boston: 2012.

Paulson OB, Strandgaard S, Edvinsson L. Cerebral autoregulation. Cerebrovasc Brain Metab Rev. 1990; 2:161–192. [PubMed: 2201348]

Pescatello LS, Fargo AE, Leach CN, Scherzer HH. Short-term effect of dynamic exercise on arterial blood pressure. Circulation. 1991; 83:1557–1561. [PubMed: 2022015]

Poublanc J, Han JS, Mandell DM, Conklin J, Stainsby JA, Fisher JA, Mikulis DJ, Crawley AP. Vascular steal explains early paradoxical blood oxygen level-dependent cerebrovascular response in brain regions with delayed arterial transit times. Cerebrovasc Dis Extra. 2013; 3:55–64. [PubMed: 24052795]

Poulin MJ, Liang PJ, Robbins PA. Dynamics of the cerebral blood flow response to step changes in endtidal $PCO_2$ and $PO_2$ in humans. J Appl Physiol. 1996; 81:1084–1095. [PubMed: 8889738]

Prisman E, Slessarev M, Han J, Poublanc J, Mardimae A, Crawley A, Fisher J, Mikulis D. Comparison of the effects of independently-controlled endtidal $PCO_2$ and $PO_2$ on blood oxygen level-dependent (BOLD) fMRI. J Magn Reson Imaging. 2008; 27:185–191. [PubMed: 18050321]

Rack-Gomer AL, Liu TT. Caffeine increases the temporal variability of resting-state BOLD connectivity in the motor cortex. NeuroImage. 2012; 59:2994–3002. [PubMed: 22032947]

Regan RE, Fisher JA, Duffin J. Factors affecting the determination of cerebrovascular reactivity. Brain Behav. 2014; 4:775–788. [PubMed: 25328852]

Robbins PA, Conway J, Cunningham DA, Khamnei S, Paterson DJ. A comparison of indirect methods for continuous estimation of arterial $PCO_2$ in men. J Appl Physiol. 1990; 68:1727–1731. [PubMed: 2112130]

Scuteri AA, Brancati AMA, Gianni WW, Assisi AA, Volpe MM. Arterial stiffness is an independent risk factor for cognitive impairment in the elderly: a pilot study. J Hypertens. 2005; 23:1211–1216. [PubMed: 15894897]

Sesso HD, Stampfer MJ, Rosner B, Hennekens CH, Gaziano JM, Manson JE, Glynn RJ. Systolic and diastolic blood pressure, pulse pressure, and mean arterial pressure as predictors of cardiovascular disease risk in men. Hypertension. 2000; 36:801–807. [PubMed: 11082146]

Slessarev M, Han J, Mardimae A, Prisman E, Preiss D, Volgyesi G, Ansel C, Duffin J, Fisher JA. Prospective targeting and control of endtidal $CO_2$ and $O_2$ concentrations. J Physiol. 2007; 581:1207–1219. [PubMed: 17446225]

Sobczyk O, Battisti-Charbonney A, Fierstra J, Mandell DM, Poublanc J, Crawley AP, Mikulis DJ, Duffin J, Fisher JA. A conceptual model for $CO_2$-induced redistribution of cerebral blood flow with experimental confirmation using BOLD MRI. NeuroImage. 2014; 92:56–68. [PubMed: 24508647]

Sousa I, Vilela P, Figueiredo P. Reproducibility of hypocapnic cerebrovascular reactivity measurements using BOLD fMRI in combination with a paced deep breathing task. NeuroImage. 2014; 98:31–41. [PubMed: 24769177]

Spano VR, Mandell DM, Poublanc J, Sam K, Battisti-Charbonney A, Pucci O, Han JS, Crawley AP, Fisher JA, Mikulis DJ. $CO_2$ blood oxygen level-dependent MR mapping of cerebrovascular reserve in a clinical population: safety, tolerability, and technical feasibility. Radiology. 2013; 266:592–598. [PubMed: 23204541]

Stefanovic B, Warnking JM, Rylander KM, Pike GB. The effect of global cerebral vasodilation on focal activation hemodynamics. NeuroImage. 2006; 30:726–734. [PubMed: 16337135]

Sun, P., Yan, H., Ranadive, S., Lane, A., Kappus, R., Bunsawat, K., Baynard, T., Li, S., Fernhall, B. Blood pressure changes following aerobic exercise in Caucasian and Chinese descendants. Int J Sports Med. 2014. http://dx.doi.org/10.1055/s-0034-1390493 (Epub ahead of print)

Suri S, Mackay CE, Kelly ME, Germuska M, Tunbridge EM, Frisoni GB, Matthews PM, Ebmeier KP, Bulte DP, Filippini N. Reduced cerebrovascular reactivity in young adults carrying the APOE epsilon4 allele. Alzheimers Dement. 2014

Tak S, Wang DJJ, Polimeni JR, Chen JJ. Dynamic and static contributions of the cerebrovasculature to the resting-state BOLD signal. NeuroImage. 2014; 84C:672–680.

Tancredi FB, Hoge RD. Comparison of cerebral vascular reactivity measures obtained using breath-holding and $CO_2$ inhalation. J Cereb Blood Flow Metab. 2013; 33:1066–1074. [PubMed: 23571282]

Tancredi FB, Gauthier CJ, Madjar C, Bolar DS, Fisher JA, Wang DJJ, Hoge RD. Comparison of pulsed and pseudocontinuous arterial spin-labeling for measuring $CO_2$-induced cerebrovascular reactivity. J Magn Reson Imaging. 2012; 36:312–321. [PubMed: 22544711]

Tarumi T, Ayaz Khan M, Liu J, Tseng BY, Parker R, Riley J, Tinajero C, Zhang R. Cerebral hemodynamics in normal aging: central artery stiffness, wave reflection, and pressure pulsatility. J Cereb Blood Flow Metab. 2014; 34:971–978. [PubMed: 24643081]

Thomas BP, Liu P, Park DC, van Osch MJ, Lu H. Cerebrovascular reactivity in the brain white matter: magnitude, temporal characteristics, and age effects. J Cereb Blood Flow Metab. 2014; 34:242–247. [PubMed: 24192640]

Tukey, JW. Exploratory Data Analysis. Addison-Wesley; 1977.

van Elderen SG, Brandts A, van der Grond J, Westenberg JJ, Kroft LJ, van Buchem MA, Smit JW, de Roos A. Cerebral perfusion and aortic stiffness are independent predictors of white matter brain atrophy in type 1 diabetic patients assessed with magnetic resonance imaging. Diabetes Care. 2011; 34:459–463. [PubMed: 21216862]

van Popele NM, Grobbee DE, Bots ML, Asmar R, Topouchian J, Reneman RS, Hoeks AP, van der Kuip DA, Hofman A, Witterman JC. Association between arterial stiffness and atherosclerosis: the Rotterdam Study. Stroke. 2001; 32:454–460. [PubMed: 11157182]

Vesely A, Sasano H, Volgyesi G, Somogyi R, Tesler J, Fedorko L, Grynspan J, Crawley A, Fisher JA, Mikulis D. MRI mapping of cerebrovascular reactivity using square wave changes in end-tidal $PCO_2$. Magn Reson Med. 2001; 45:1011–1013. [PubMed: 11378878]

Wu WC, Wong EC. Intravascular effect in velocity-selective arterial spin labeling: the choice of inflow time and cutoff velocity. NeuroImage. 2006; 32:122–128. [PubMed: 16713716]

Yezhuvath US, Lewis-Amezcua K, Varghese R, Xiao G, Lu H. On the assessment of cerebrovascular reactivity using hypercapnia BOLD fMRI. NMR Biomed. 2009; 22:779–786. [PubMed: 19388006]

Zhao P, Alsop DC, Abduljalil A, Selim M, Lipsitz L, Novak P, Caplan L, Hu K, Novak V. Vasoreactivity and peri-infarct hyperintensities in stroke. Neurology. 2009; 72:643–649. [PubMed: 19221298]

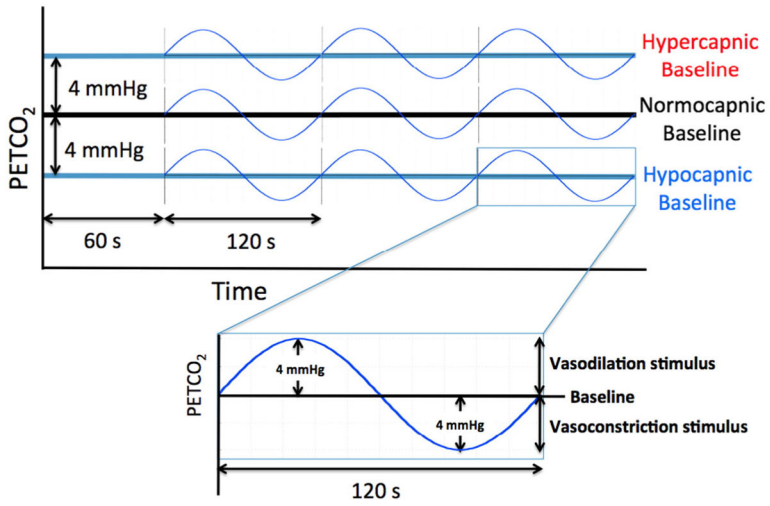


**Fig. 1. The experimental paradigm**

$PETCO_2$ was sinusoidally modulated with a period of 120 s; 3 periods of sinusoidal $PETCO_2$ variations were induced, following a 1-minute baseline. This bipolar stimulus includes both vasodilatory (upper half of sinusoid) and vasoconstrictive (bottom half of sinusoid) components. This sinusoidal manipulation was applied at the subject's natural baseline (normocapnic) as well as at hypercapnic and hypocapnic baselines, which are separated from the normocapnic baseline by 4 mm Hg.

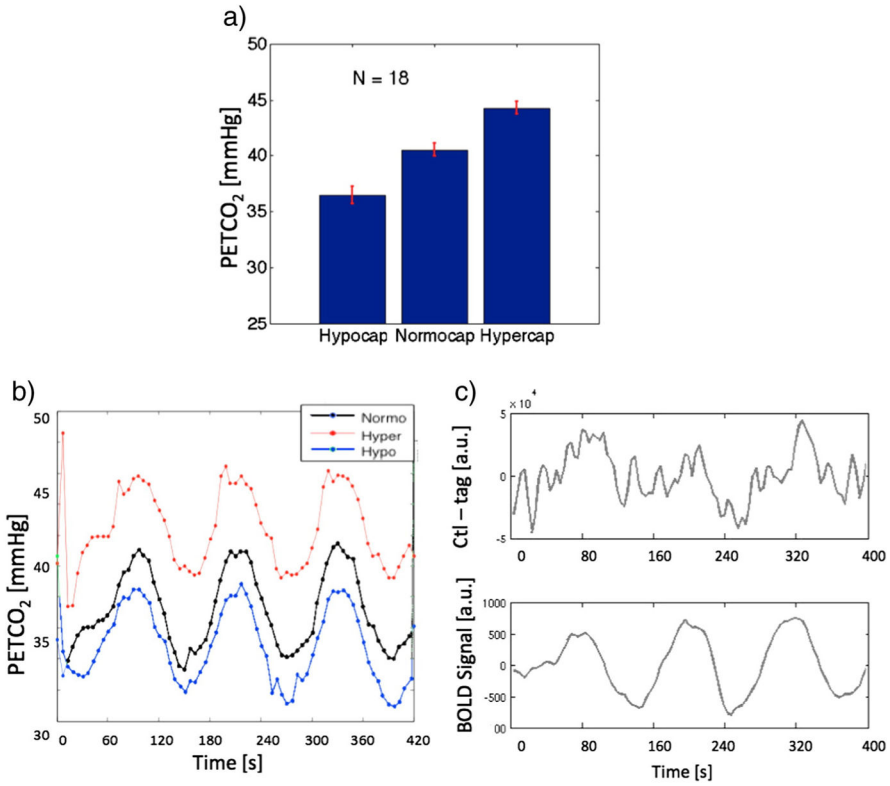


**Fig. 2. Sample $PETCO_2$ and fMRI data**

(a) The $PETCO_2$ levels corresponding to the three vascular tension levels are shown with error bars indicating standard error across subjects. (b) Prospective targeting permitted us to realize our designated $PETCO_2$ changes of approximately 4 mm Hg in either direction, relative to the participant's natural baseline. (c) The sinusoidal $PETCO_2$ modulation (b) induced robust CBF and BOLD signal changes.

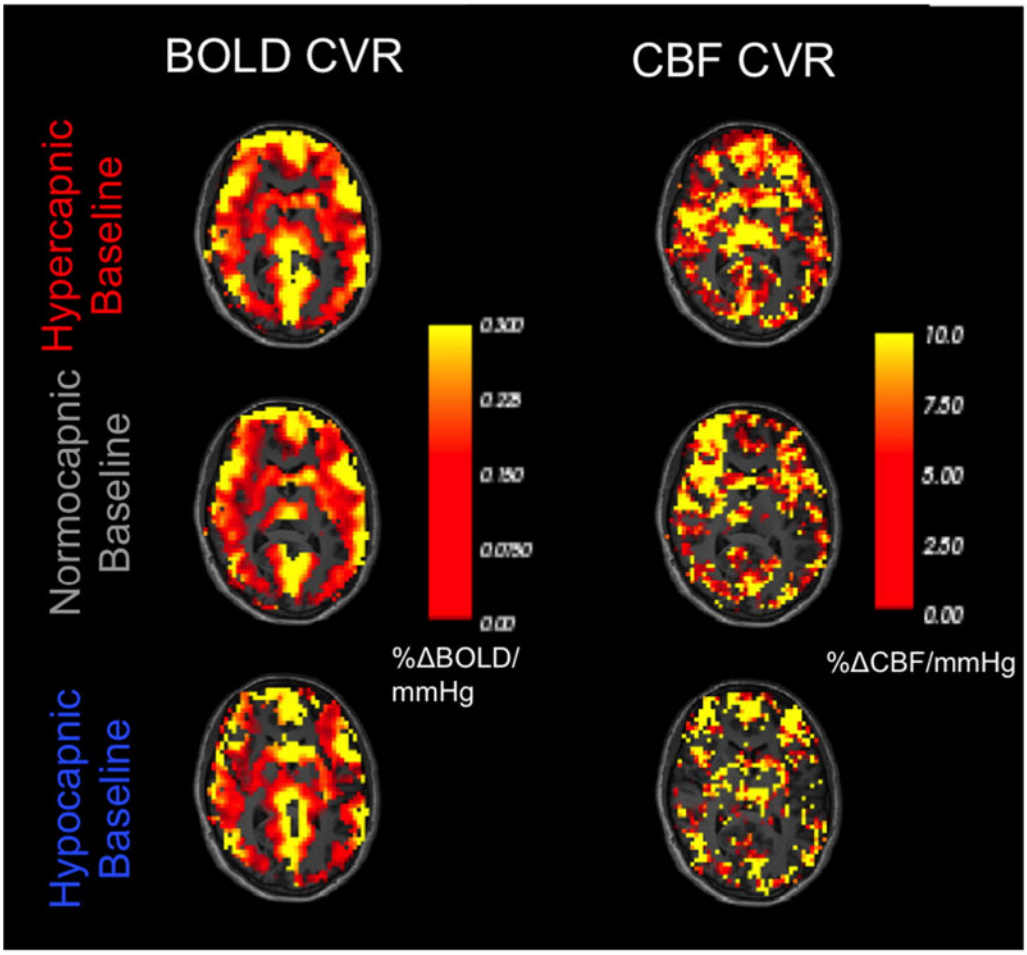


**Fig. 3. Sample BOLD and CBF CVR maps across all vascular tension levels**

BOLD-based CVR maps in response to the bipolar sinusoidal stimulus. Qualitatively lower signal-to-noise ratios (SNRs) can be discerned in the CBF-based CVR maps compared to the BOLD, and the response at the hypocapnic (preconstricted) baseline appears to be the lowest compared to the other two basal vascular tension levels.

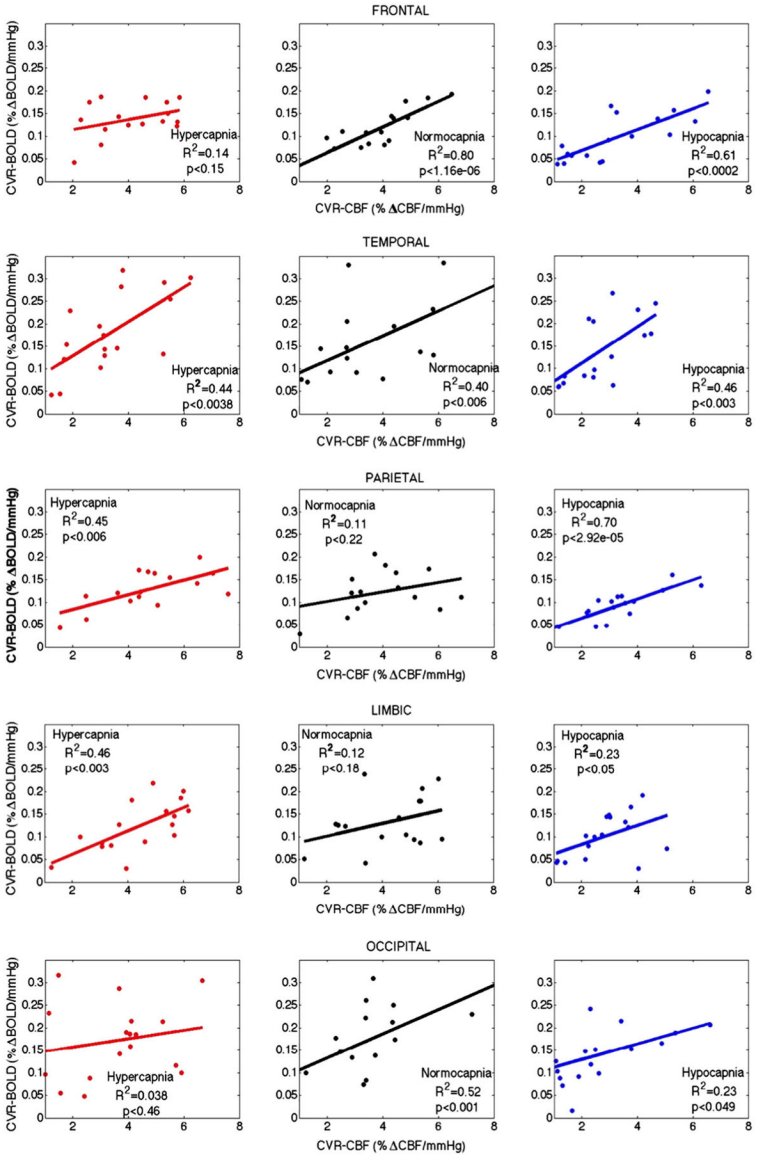


**Fig. 4. The relationship between BOLD- and CBF-based CVR measurements across main regions-of-interest (ROIs)**

Red, black and blue represent hypercapnic, normocapnic and hypocapnic baselines, respectively. In most regions, the BOLD and CBF CVR values were significantly correlated. Note that the plotted values correspond to regional averages prior to ROI-outlier removal.

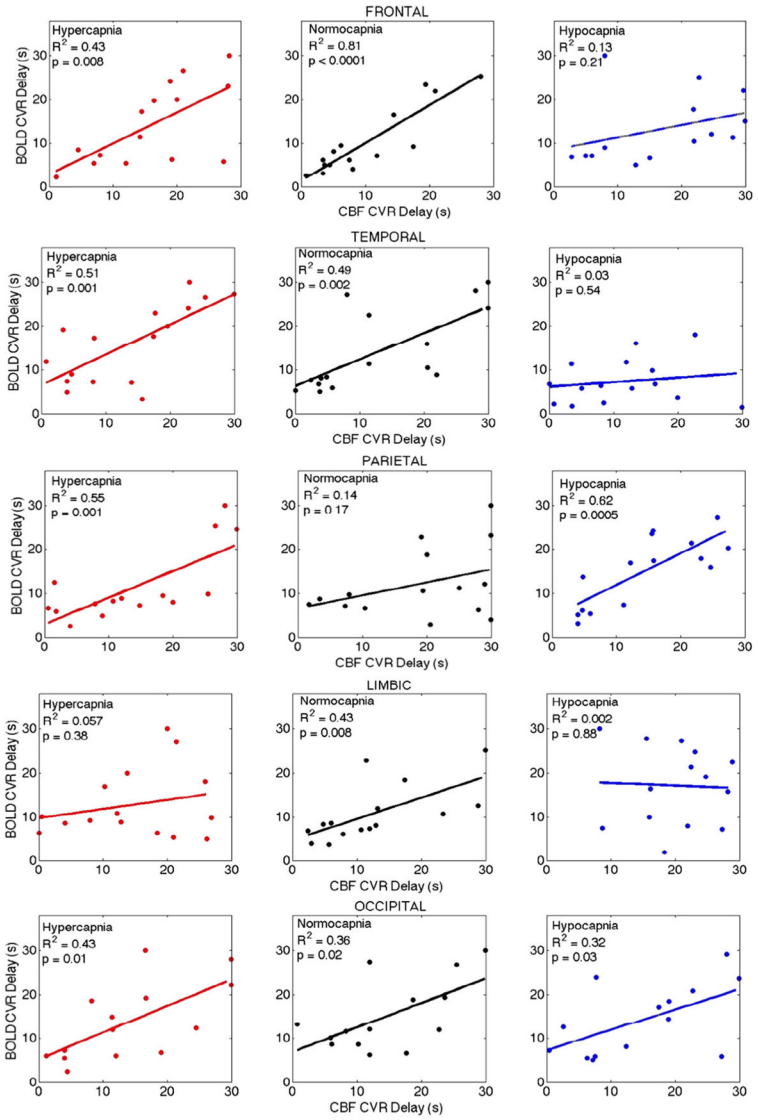


**Fig. 5. Relationship between BOLD- and CBF-based CVR delay measurements across ROIs**

Again, red, black and blue represent hypercapnic, normocapnic and hypocapnic baselines, respectively. The BOLD and CBF CVR delay values were significantly correlated in most brain regions.

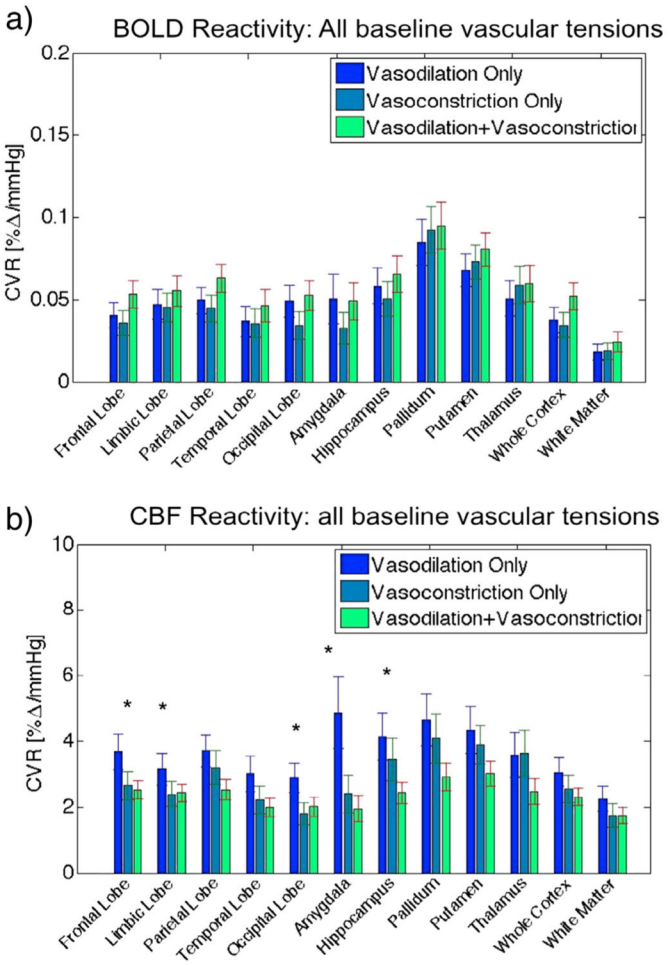


**Fig. 6. The dependence of BOLD and CBF CVR measurements on the type of vascular stimulus**

Compared to CBF measurements, BOLD measurements of CVR were insensitive to the type of stimulus employed. The asterisks indicate statistically significant trends and differences (based on ANOVA results). The plotted values correspond to regional averages after ROI-outlier removal.

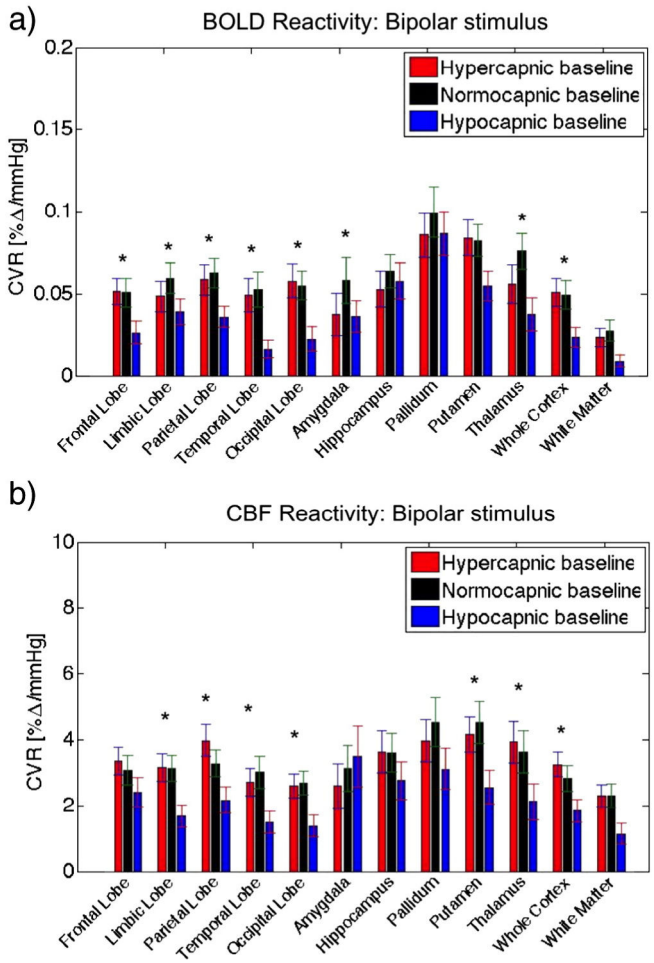


**Fig. 7. The dependence of BOLD and CBF CVR measurements on vascular baseline (basal vascular tension): bipolar stimulus**

BOLD and CBF were similarly sensitive to vascular tension, although different behaviors are observed. The asterisks indicate statistically significant trends and differences (based on ANOVA results). The plotted values correspond to regional averages after ROI-outlier removal.

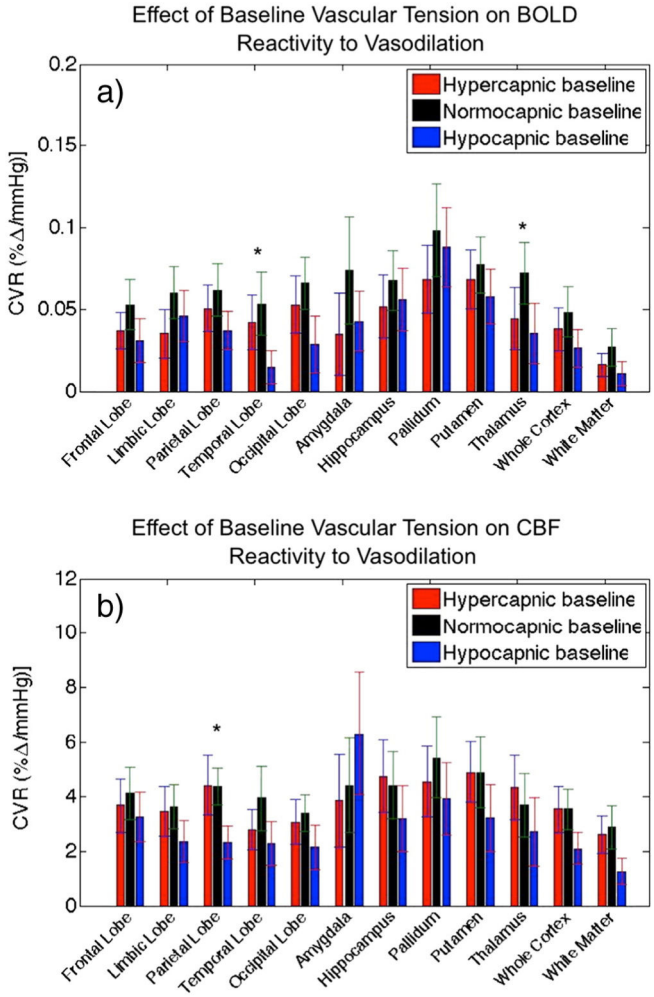


**Fig. 8. The dependence of BOLD and CBF CVR measurements on vascular baseline (basal vascular tension): vasodilatory stimulus**

The normocapnic (resting) baseline was generally associated with a higher BOLD response to vasodilatory stimulation, while the effect is much less pronounced in CBF. The asterisks indicate statistically significant trends and differences (based on ANOVA results). The plotted values correspond to regional averages after ROI-outlier removal.

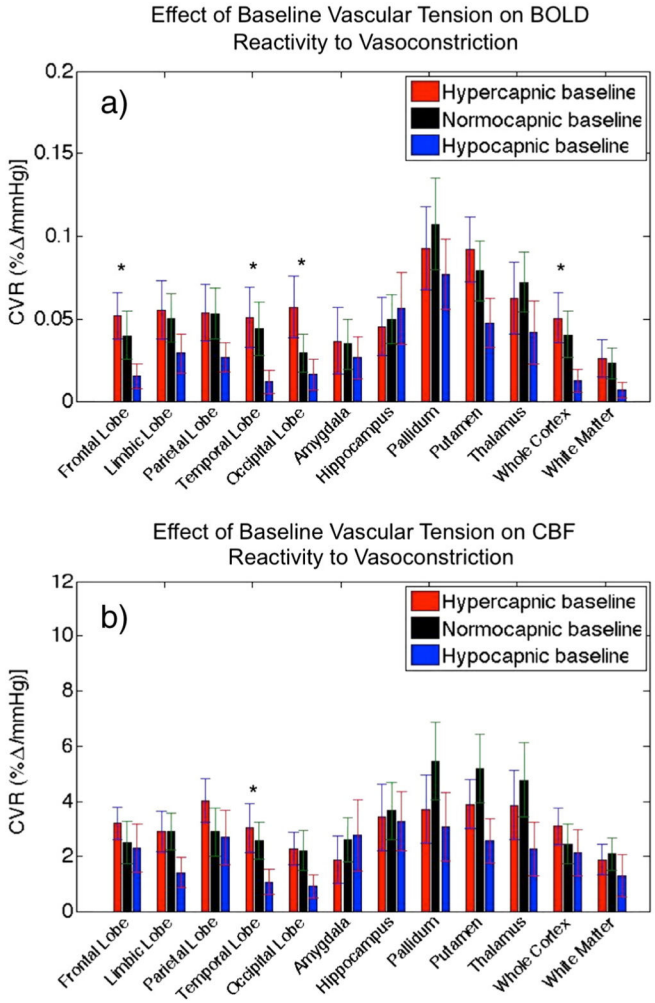


**Fig. 9. The dependence of BOLD and CBF CVR measurements on vascular baseline (basal vascular tension): vasoconstrictive stimulus**

For both BOLD and CBF, the hypercapnic (predilated) baseline was associated with a higher CVR. The asterisks indicate statistically significant trends and differences (based on ANOVA results). The plotted values correspond to regional averages after ROI-outlier removal.

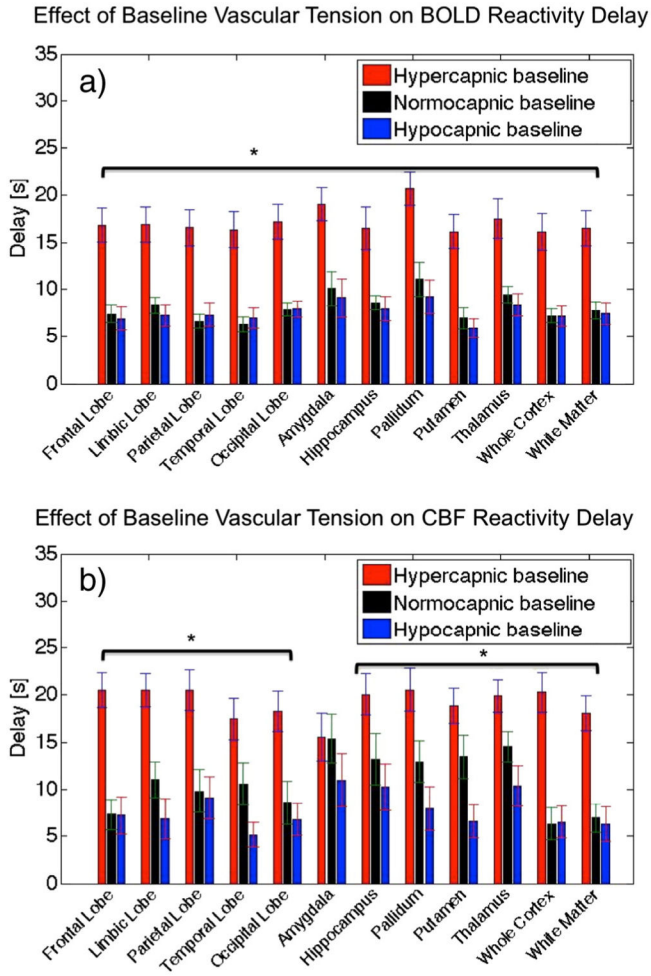


**Fig. 10. The dependence of BOLD and CBF CVR delay measurements on vascular baseline (basal vascular tension)**

For both BOLD and CBF, the predilated (hypercapnic) baseline was associated with the longest $CO_2$ response delays. The asterisks indicate statistically significant trends and differences (based on ANOVA results). The plotted values correspond to regional averages after ROI-outlier removal.

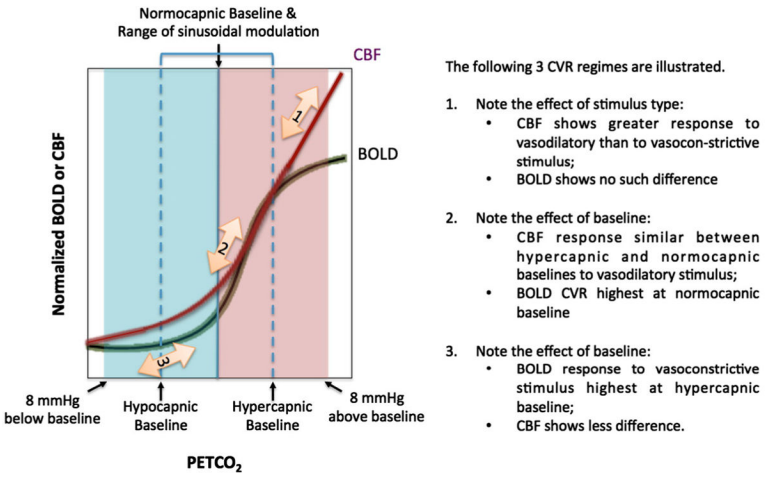


**Fig. 11. Conceptualized illustration of CVR measurement dependence on basal vascular tension**

The key features of the plots are marked with numbers, and explained in the right half of the figure. The blue and pink shading represent the $PETCO_2$ spans associated with the sinusoidal manipulation at the hypocapnic (preconstricted) and hypercapnic (predilated) baselines, respectively. In this work, BOLD-based response to the vasodilatory stimulus was lower at hypercapnic baseline compared to normocapnic baseline, consistent with a nonlinear BOLD response to changing baseline $PETCO_2$. However, CBF maintained a larger linear range with increasing $PETCO_2$.

## Table 1

**The dependence of CVR estimate amplitude on basal vascular tension and the type of vascular challenge**

Summarized here are assessments by the multi-variate ANOVA. We did not find significant interactions between vascular tension and the type of vascular stimulus.

| | BOLD | CBF |
|---|---|---|
| *Effect of vascular stimulus type* | | |
| Cortex | – | Frontal lobe (p = 0.05) |
| | | Temporal lobe (p = 0.04) |
| | | Occipital lobe (p = 0.04) |
| Subcortex | – | Hippocampus (p = 0.05) |
| | | Amygdala (p = 0.01) |
| White matter | – | – |
| *Effect of basal vascular tension: bipolar stimulus* | | |
| Cortex | Frontal lobe (p = 0.04) | Limbic lobe (p = 0.008) |
| | Limbic lobe (p = 0.04) | Parietal lobe (p = 0.01) |
| | Parietal lobe (p = 0.05) | Temporal lobe (p = 0.02) |
| | Temporal lobe (p = 0.009) | Occipital lobe (p = 0.01) |
| | Occipital lobe (p = 0.009) | Whole cortex (p = 0.02) |
| | Whole cortex (p = 0.02) | |
| Subcortex | Amygdala (p = 0.05) | Putamen (p = 0.03) |
| | Thalamus (p = 0.05) | Thalamus (p = 0.05) |
| White matter | All regions (p = 0.04) | All regions (p = 0.02) |
| *Effect of vascular tension: vasodilatory stimulus* | | |
| Cortex | Temporal lobe (p = 0.05) | Parietal lobe (p = 0.05) |
| Subcortex | Thalamus (p = 0.01) | – |
| White matter | – | – |
| Effect of vascular tension: vasoconstrictive stimulus | | |
| Cortex | Frontal lobe (p = 0.05) | Temporal lobe (p = 0.05) |
| | Temporal lobe (p = 0.05) | |
| | Occipital lobe (p = 0.04) | |
| | Whole cortex (p = 0.05) | |
| Subcortex | – | – |
| White matter | – | – |

**Table 2**

**The dependence of CVR delay estimates on baseline vascular tone**

assessment by univariate ANOVA.

| Effect of basal vascular tone | BOLD | CBF |
|---|---|---|
| Cortex | Frontal lobe (p = 2e-6) | Frontal lobe (p = 2e-5) |
| | Limbic lobe (p = 7e-7) | Limbic lobe (p = 3e-5) |
| | Parietal lobe (p = 3e-6) | Parietal lobe (p = 0.0008) |
| | Temporal lobe (p = 2e-7) | Temporal lobe (p = 0.0003) |
| | Occipital lobe (p = 4e-8) | Occipital lobe (p = 0.0005) |
| Subcortex | Amygdala (p = 0.0006) | Hippocampus (p = 0.002) |
| | Hippocampus (p = 4e-6) | Pallidum (p = _0.001) |
| | Pallidum (p = 6e-5) | Putamen (p = _0.0003) |
| | Putamen (p = 7e-6) | Thalamus (p = 0.0002) |
| | Thalamus (p = 5e-6) | |
| White matter | All regions (p = 2e-6) | All regions (p = 5e-7) |